



Interictal network synchrony and local heterogeneity predict epilepsy surgery outcome among pediatric patients

*†Samuel B. Tomlinson, ‡Brenda E. Porter, and *§Eric D. Marsh

Epilepsia, 58(3):402–411, 2017
doi: 10.1111/epi.13657

SUMMARY

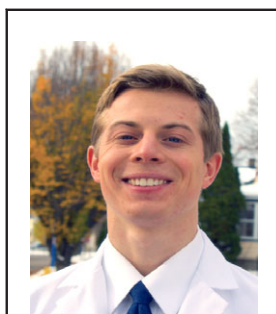
Objective: Epilepsy is a disorder of aberrant cortical networks. Researchers have proposed that characterizing presurgical network connectivity may improve the surgical management of intractable seizures, but few studies have rigorously examined the relationship between network activity and surgical outcome. In this study, we assessed whether local and global measures of network activity differentiated patients with favorable (seizure-free) versus unfavorable (seizure-persistent) surgical outcomes.

Methods: Seventeen pediatric intracranial electroencephalography (IEEG) patients were retrospectively examined. For each patient, 1,200 random interictal epochs of 1-s duration were analyzed. Functional connectivity networks were constructed using an amplitude-based correlation technique (Spearman correlation). Global network synchrony was computed as the average pairwise connectivity strength. Local signal heterogeneity was defined for each channel as the variability of EEG amplitude (root mean square) and absolute delta power ($\mu\text{V}^2/\text{Hz}$) across epochs. A support vector machine learning algorithm used global and local measures to classify patients by surgical outcome. Classification was assessed using the Leave-One-Out (LOO) permutation test.

Results: Global synchrony was increased in the seizure-persistent group compared to seizure-free patients (Student's *t*-test, $p = 0.006$). Seizure-onset zone (SOZ) electrodes exhibited increased signal heterogeneity compared to non-SOZ electrodes, primarily in seizure-persistent patients. Global synchrony and local heterogeneity measures were used to accurately classify 16 (94.1%) of 17 patients by surgical outcome (LOO test, iterations = 10,000, $p < 0.001$).

Significance: Measures of global network synchrony and local signal heterogeneity represent promising biomarkers for assessing patient candidacy in pediatric epilepsy surgery.

KEY WORDS: Epilepsy surgery, Epileptogenic zone, Pediatric epilepsy, Intracranial EEG, Functional connectivity.



Samuel Tomlinson is pursuing an M.D. degree at the University of Rochester School of Medicine and Dentistry.

Intractable epilepsy is a debilitating neurologic condition that reduces quality of life and increases morbidity among affected individuals. Although the precise pathophysiologic mechanisms of epilepsy are unclear in most cases, epilepsy is increasingly understood as a disorder of aberrant cortical

networks.^{1,2} In the healthy state, the balance of excitation and inhibition in cortical networks is tightly regulated to facilitate communication between remote functional centers.³ Neocortical seizures are thought to arise when activity becomes excessively synchronized within the *epileptogenic*

Accepted November 28, 2016; Early View publication February 6, 2017.

*Division of Child Neurology, Department of Pediatrics, Children's Hospital of Philadelphia, Philadelphia, Pennsylvania, U.S.A.; †School of Medicine and Dentistry, University of Rochester Medical Center, Rochester, New York, U.S.A.; ‡Department of Neurology and Neurological Science, Stanford School of Medicine, Palo Alto, California, U.S.A.; and §Department of Neurology, Perelman School of Medicine, University of Pennsylvania, Philadelphia, Pennsylvania, U.S.A.

Address correspondence to Eric D. Marsh, Division of Child Neurology, Department of Pediatrics, Children's Hospital of Philadelphia, Abramson Research Building, Room 502E, 3615 Civic Center Boulevard, Philadelphia, PA 19014, U.S.A. E-mail: marshe@email.chop.edu

Wiley Periodicals, Inc.

© 2017 International League Against Epilepsy

KEY POINTS

- Interictal network activity was characterized in pediatric epilepsy surgery patients
- Global synchrony and local heterogeneity measures accurately predicted surgical outcome
- Interictal network synchrony may be useful for prospectively assessing surgical candidacy

zone, or the network of structures responsible for generating and transmitting epileptic seizures.^{4,5} For most patients, pharmacotherapy is sufficient to control excitation within the epileptogenic zone.⁶ However, approximately one third of patients develop medically refractory seizures that may be amenable to surgical intervention.⁷ Epilepsy surgery has proven efficacy in reducing seizure frequency, enhancing perceptions of self-worth, and improving neurodevelopmental outcomes for many patients.⁸ Unfortunately, a high percentage of pediatric patients (~40% for extratemporal lobe epilepsies) have unfavorable surgical outcomes marked by persistent seizures and/or functional deficits.⁹

Intracranial EEG (IEEG) is a clinical procedure in which electrical activity is sampled directly from the cortex with relatively high spatial and temporal resolution.¹⁰ Although IIEG recordings are traditionally assessed by visual inspection, recent advances in computing power and automated IIEG techniques have allowed researchers to study cortical synchronization across visually inaccessible spatiotemporal scales. At the global (i.e., multi-electrode) scale, *functional connectivity* encodes the statistical similarity of electrical events between all pairs of electrodes, thereby measuring synchronized activity across distributed cortical networks.¹¹ At the local (i.e., single-electrode) level, synchrony within local neuronal populations can be characterized by the signal amplitude and/or the distribution of power across the frequency spectrum. In epilepsy, alterations in local signal features and global network synchrony are routinely observed in the between-seizure (i.e., interictal) state, and past studies have shown that the removal of hypersynchronous regions correlates with favorable surgical outcomes.^{12,13}

In a recent study, researchers characterized functional connectivity in 23 adult temporal lobe epilepsy (TLE) patients, finding that a simple analysis of global network connectivity was sufficient to predict surgical outcome with 87% accuracy.¹⁴ This study raises the possibility of using interictal network measures as prospective biomarkers for assessing surgical candidacy, which would transform the surgical management of intractable seizures. Although the findings of Antony et al.¹⁴ hold tremendous promise, further investigation is needed to define the clinical utility of the approach. The purpose of this study was

to examine the relationship between interictal connectivity networks, cortical synchrony, and surgical outcome in a group of pediatric IIEG patients. As a global measure of network synchrony, we extracted functional connectivity networks and determined the mean connectivity strength across electrode pairs. To describe activity at the local scale, we examined the variability (i.e., “heterogeneity”) of EEG amplitude and absolute delta power (0–4 Hz, $\mu\text{V}^2/\text{Hz}$) across epochs and compared signal heterogeneity between seizure-onset zone (SOZ) and non-SOZ electrodes. We hypothesized that global network synchrony and local signal heterogeneity would reliably differentiate patients with favorable (seizure-free) versus unfavorable (seizure-persistent) surgical outcomes.

METHODS

Clinical data

The Children’s Hospital of Philadelphia (CHOP) Institutional Review Board approved this study. Recordings were analyzed retrospectively from 17 patients who underwent phase II presurgical IIEG evaluation at CHOP between the years of 2002 and 2009. Patients were selected based on the availability of spatial electrode maps, detailed seizure markings, and limited presence of IIEG artifact. Implant decisions were not influenced by this study, and consent was obtained from each patient’s family prior to inclusion. Review of patient charts provided descriptions of implantation site, histopathology, magnetic resonance imaging (MRI) description, and epilepsy history. Surgical outcomes were assessed by primary neurologists at last patient contact (minimum postoperative duration = 2 years) using the modified Engel classification system:¹⁵ class I, seizure-free; class II, significant improvement; class III, worthwhile improvement; and class IV, no improvement. Patients with Engel class I were assigned to the seizure-free group (Sz-Free, $n = 9$), whereas patients with Engel class \geq II were assigned to the seizure-persistent group (Sz-Persist, $n = 8$).

EEG acquisition

Clinical recordings were acquired at 200 Hz using a Telefactor Beehive 32–128 channel Cable Telemetry Encoder (CTE) digital synchronized video-EEG recording system with 16-bit amplifiers (Astro Med Corp, West Warwick, RI, U.S.A.). Subdural grids and strips with embedded platinum electrodes (2.3 mm exposure, 10 mm spacing) were used for all patients (Adtech Medical Instrument Corporations, Racine, WI, U.S.A.). Data were subjected online to 60 Hz notch filtering, and voltages were referenced online to an epidural electrode strip distant from the suspected epileptogenic region. Two experienced pediatric epileptologists (EDM; BEP) visually inspected each patient’s entire IIEG recording for seizures and independently marked the following parameters: (1) time of earliest electrographic change at seizure onset; (2) time of unequivocal seizure

offset; and (3) the SOZ channels. Consensus between the IEEG readers defined the SOZ for use in later analyses.

EEG segmentation

For each patient, 1,200 non-overlapping interictal segments of 1-s duration (total IEEG per patient = 20 min) were extracted randomly from the IEEG record (Fig. 1A). The epoch duration was chosen for consistency with previous studies and to balance the conflicting demands of signal quasi-stationarity and sufficient data samples.¹⁶ Epochs were selected to occur at least 10 min from the nearest seizure and were not screened by time-of-day or physiologic state. Epochs were filtered (0–50 Hz) offline using a finite-impulse response (FIR), phase-invariant digital filter implemented in EEGLAB v13.5.4b.¹⁷ A combination of custom MATLAB 2016a scripts (Mathworks, Natick, MA, U.S.A.) and EEGLAB plug-ins facilitated manual inspection of filtered epochs. A reviewer (SBT) blinded to patient and electrode identity discarded epochs containing excessive artifact and marked channels with persistent electrical noise for exclusion.

Functional connectivity

Functional connectivity was calculated using the zero-lag Spearman rank correlation coefficient between all possible electrode pairs (Eq. A1.1). Pairwise correlations (ranging from -1 to 1) were computed within each epoch (Fig. 1A) and averaged across epochs to obtain a single *channel-by-channel* connectivity matrix per patient (Fig. 1B). Because Spearman coefficients are non-normally distributed, raw correlation values were normalized by Fisher-Z transformation prior to cross-epoch averaging.¹⁸ Entries along the diagonal (i.e., self-connections) were forced to 0. The Spearman correlation was favored in this study because it is

a nonparametric measure that captures both linear and non-linear relationships.¹⁸

Global network synchrony

Two approaches were used to characterize global synchrony within functional connectivity matrices. First, the average of the off-diagonal matrix entries (i.e., mean connectivity strength) was computed and compared across outcome groups using two-tailed Student's *t*-tests.¹⁴ Then, the cumulative probability distribution (CPD) of edge weights (i.e., connection strengths) for each patient's functional connectivity matrix was calculated (edge weight increment = 0.005). The average CPD curves for Sz-Free and Sz-Persist groups were compared using the nonparametric Functional Data Analysis (FDA) technique detailed elsewhere,¹⁹ with surrogate iterations (*k*) set to *k* = 10,000.

The issue of interictal spikes influencing functional connectivity measures has been raised in multiple studies.^{20,21} In this study, we used an automated spike detection algorithm developed previously by our group²² and validated against expert pediatric epileptologists to characterize spike activity. For each patient, full-duration interictal EEG recordings were submitted to the spike detector, and 10 segments of 10,000 interictal spikes were randomly extracted for calculation of interictal spike density (spikes/channel/min) (Tomlinson SB, et al., *Frontiers in Neurology*). Correlation analysis was then performed to evaluate the relationship between interictal spike density and global connectivity strength.

Local signal heterogeneity

Local signal heterogeneity refers to the variability of EEG signals across epochs at each electrode contact. In this study, two measures of local heterogeneity were examined:

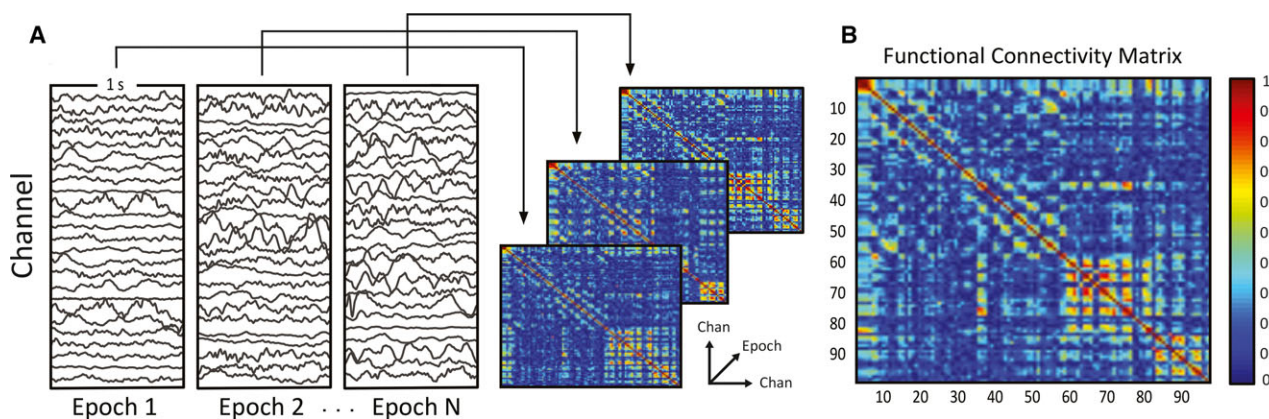


Figure 1.

Construction of functional connectivity networks. (A) Left: Three representative 1-s epochs from patient 13 are shown (electrodes plotted = 25). Right: Functional connectivity matrices were derived for each epoch via the zero-lag Spearman rank correlation coefficient. Because the Spearman correlation is an undirected measure, connectivity matrices are symmetric about the diagonal. (B) Pairwise correlation coefficients were averaged across epochs to generate a single *channel-by-channel* functional connectivity matrix per patient. The mean and cumulative probability distribution (CPD) of off-diagonal matrix entries were used to characterize global network synchrony.

Epilepsia © ILAE

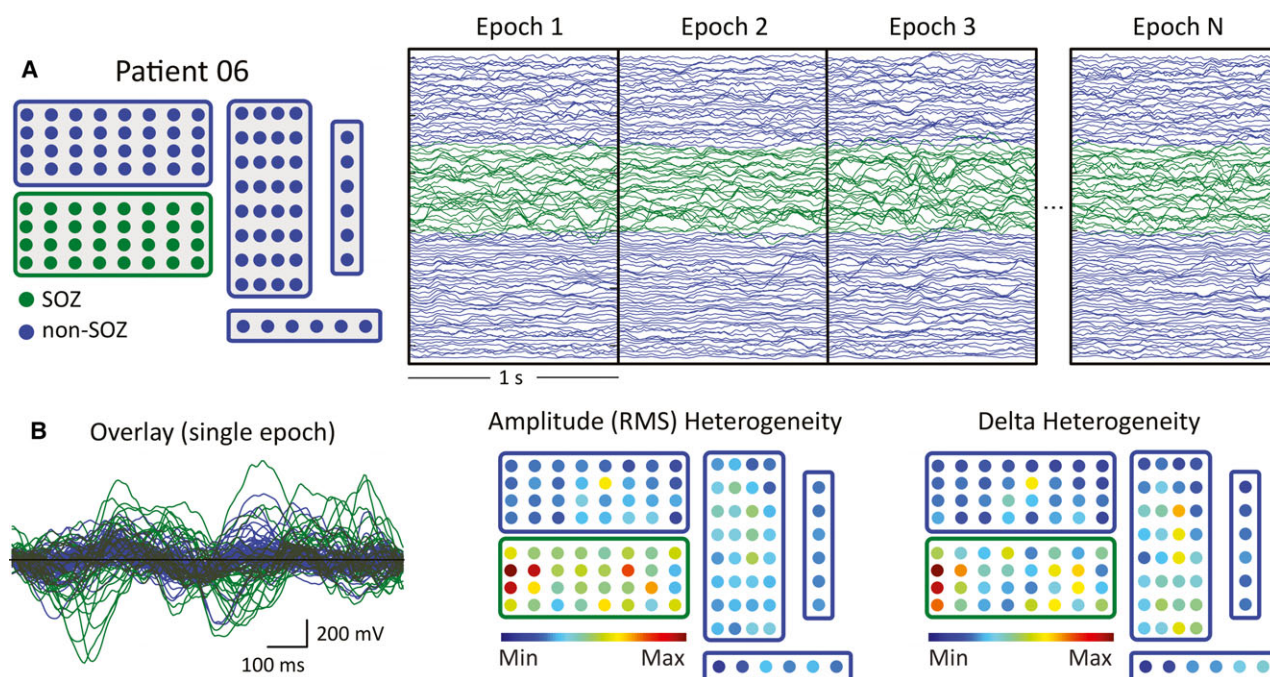


Figure 2.

Local signal heterogeneity procedure demonstrated for a representative patient. **(A)** Left: The implant schematic for patient 06 is shown (electrodes = 108). Green electrodes correspond to the SOZ, whereas blue electrodes correspond to non-SOZ channels. Right: Four representative 1-s epochs with SOZ channels colored in green. **(B)** Left: Trace overlay from epoch 1 reveals increased high-amplitude slow-wave activity in SOZ channels. Middle and right: The channel-wise heterogeneity (standard deviation) of signal amplitude (root mean square, RMS) and absolute delta power ($\mu\text{V}^2/\text{Hz}$) were computed. For this patient, channel-wise heat maps reveal increased amplitude heterogeneity and delta heterogeneity within SOZ compared to non-SOZ electrodes.

Epilepsia © ILAE

the signal amplitude (root mean square, RMS), and the absolute spectral power ($\mu\text{V}^2/\text{Hz}$) in the delta frequency range (0–4 Hz) (Fig. 2). Emphasis on these two signal features was motivated by previous studies finding increased interictal RMS amplitude²⁰ and regional delta power²³ within SOZ channels. Thus, the goal of this analysis was to compare patterns of local signal heterogeneity in SOZ and non-SOZ electrodes.

To quantify local signal heterogeneity, epochs were first de-trended (linear) to mitigate variability introduced by electrode impedance and implant location.²⁰ The channel-wise RMS amplitude was then computed within each epoch (Eq. A1.2). Amplitude heterogeneity was computed for each electrode by taking the standard deviation of RMS values across epochs. Epochs were then tapered with a Hamming window (duration = 1 s) and decomposed via discrete fast Fourier transformation in MATLAB (frequency resolution = 1 Hz) to obtain the power spectrum. The channel-wise absolute delta power ($\mu\text{V}^2/\text{Hz}$) was computed for each epoch by averaging power values across the 0–4 Hz frequency range. Delta heterogeneity was then computed for each electrode across epochs as above (Fig. 2B).

To compare amplitude and delta heterogeneity between SOZ and non-SOZ channels, difference scores (SOZ – non-SOZ) were computed for both measures by subtracting the

mean of SOZ channels by the mean of non-SOZ channels. This procedure yielded two measures for comparison across the surgical outcome groups. Group comparisons were conducted using the Student's *t*-tests (two-tailed) with a Bonferroni-adjusted significance threshold of $p \leq 0.025$.

Support vector machine analysis

A linear-kernel support vector machine (SVM) learning algorithm was used to determine if a combination of global synchrony and local heterogeneity measures could accurately classify patients by surgical outcome. In this study, two predictor variables (global synchrony and local heterogeneity) were used in the SVM classification. Mean connectivity strength was used as the global synchrony predictor variable. For the local heterogeneity predictor, principal components analysis (PCA) was used to collapse across the two local measures assessed in the study (i.e., amplitude and delta heterogeneity SOZ/non-SOZ difference scores). Component scores from the first principal component were then submitted as the local heterogeneity predictor variable. This process ensured that both local measures were utilized in an unbiased manner when performing patient classification. The performance of the SVM classifier was evaluated nonparametrically using the “Leave-One-Out” (LOO) technique.¹⁴

Statistical reporting

Unless otherwise specified, group statistics are presented as mean (μ) \pm standard deviation (σ), and p-values correspond to comparisons between the two surgical outcome groups (Sz-Free; Sz-Persist) using two-tailed Student's *t*-tests.

RESULTS

Clinical data

Patient characteristics are presented in Table 1. Nine patients were included in the Sz-Free group (Engel class I), whereas eight patients were assigned to the Sz-Persist group (Engel class \geq II). No differences were noted between the outcome groups in terms of resection age ($p = 0.20$), implant size ($p = 0.98$), percentage of electrodes analyzed ($p = 0.90$), epochs analyzed ($p = 0.26$), or fraction of electrodes included in the SOZ ($p = 0.84$). For most patients (16/17, 94.1%), SOZ electrodes were distributed across multiple implanted grids and strips. Focal cortical dysplasia (FCD) was the most common histopathologic diagnosis in the cohort ($n = 15/17$), with Taylor-Type IIa as the predominant subtype.²⁴ Of the 10 patients with FCD type IIa, 7 (70%) were members of the Sz-Persist group. The majority of Sz-Persist patients (7/8, 87.5%) had nonlesional MRI

studies, whereas the majority of Sz-Free patients (6/9, 66.7%) exhibited at least one MRI-resolvable cortical lesion (two-tailed Fisher's exact test, $p = 0.050$) (Table S1). Other variables such as epilepsy duration, seizure frequency, and implant duration were not noticeably different across groups (data not shown).

Global network synchrony

Average functional connectivity matrices for eight representative patients (four Sz-Free, four Sz-Persist) are shown in Figure 3A. Inspection of the matrices suggests that connectivity strength is increased in Sz-Persist compared to Sz-Free patients. To quantify this observation, the mean connectivity strength was computed for all patients (Fig. 3B, left). Comparison across outcome groups revealed a significant increase in mean connectivity strength among Sz-Persist (0.144 ± 0.038) compared to Sz-Free (0.092 ± 0.030) patients ($p = 0.006$). In addition, average CPDs of edge weights were significantly different between the two groups (Fig. 3B right, FDA test, iterations = 10,000, $p = 0.008$), with a rightward shift in the Sz-Persist curve indicative of increased global connectivity strength. To assess whether global connectivity measures were related to interictal spike activity, we estimated spike density (spikes/chan/min) for each patient (Table 1). No difference in interictal spike

Table 1. Clinical characteristics of the 17 patients included in the study

Patient (n = 17)	Clinical data						Epochs		Spikes		Electrodes	
	Gender	Resection age (years)	Pathology description	Engel score	Implant	Cortical lesion	Analyzed (of 1200)		Spikes/ chan/min		Analyzed (#)	SOZ (% total)
Pt 01	M	11	FCD IIb	I	RF	+	1188		0.3770		124	6.452
Pt 02	M	5	FCD IIa	3	LF	—	1194		2.9560		94	4.255
Pt 03	M	15	FCD IIa	4	RF	—	1180		6.5780		93	43.011
Pt 04	F	11	FCD IIa	4	RF	—	1144		2.3860		93	11.828
Pt 05	F	5	FCD IIa	I	LP	+	1180		5.0850		99	22.222
Pt 06	M	12	FCD IIa/ microdysgenesis	3	LF	—	1170		1.3590		106	30.189
Pt 07	M	6	FCD IIa	3	LF	—	1186		1.8080		122	21.311
Pt 08	M	8	FCD IIb	I	RF	+	1187		1.7004		86	18.605
Pt 09	F	16	FCD IIa	3	RF	+	1144		1.7160		61	26.230
Pt 10	F	3	CVA (old)	I	RF	—	1186		4.5520		105	14.286
Pt 11	M	8	FCD IIb	I	LF	+	1151		2.7390		87	47.126
Pt 12	F	14	FCD IIa	4	R Hemi	—	1187		4.8210		91	14.286
Pt 13	M	11	FCD Ib	3	RT	—	1185		2.1540		105	59.048
Pt 14	M	15	FCD IIa	I	RF	—	1167		0.3910		111	9.910
Pt 15	F	11	Ganglioglioma	I	RT	+	1179		0.9040		69	47.826
Pt 16	M	5	FCD IIa	I	LT	—	1058		1.0200		105	26.667
Pt 17	M	12	FCD IIb	I	RF	+	1035		1.7000		84	28.571
Sz-Free	N/A	8.67 ± 3.91	N/A	N/A	N/A	N/A	1147.89 ± 58.94		2.05 ± 1.74		96.67 ± 16.70	24.63 ± 14.83
Sz-Persist	N/A	11.25 ± 3.99	N/A	N/A	N/A	N/A	1173.75 ± 19.59		2.97 ± 1.81		95.63 ± 17.44	26.27 ± 17.85
p-Value	N/A	0.198	N/A	N/A	N/A	N/A	0.256		0.302		0.902	0.839

Age at time of operation ranged from 3 to 16 years (mean \pm standard deviation = 9.88 ± 4.04 years). Patients were assigned to MRI lesional (+) or MRI nonlesional (—) groups following review of MRI imaging reports. The modified Engel scale was used to quantify surgical outcome and define outcome groups (Sz-Free, Sz-Persist). Manual epoch rejection excluded an average of 39.9/1,200 epochs (3.33%). Interictal spike density (spikes/chan/min) were estimated using an automated spike detection procedure.

R, right; L, left; F, frontal; T, temporal; P, parietal; Hemi, hemisphere; SOZ, seizure-onset zone; FCD, focal cortical dysplasia (Taylor-type).

Group differences (bottom row) were assessed using Student's *t*-tests.

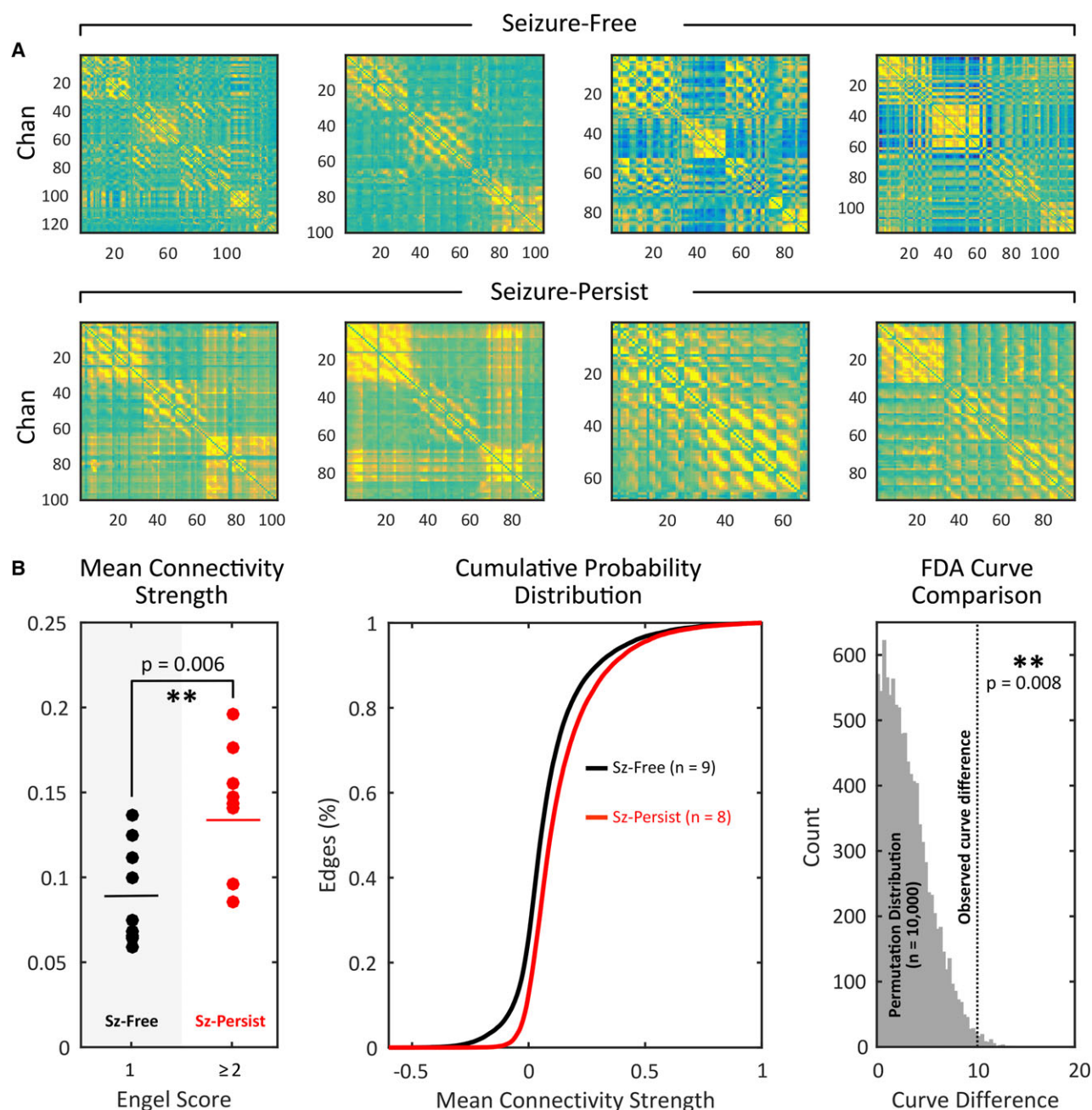


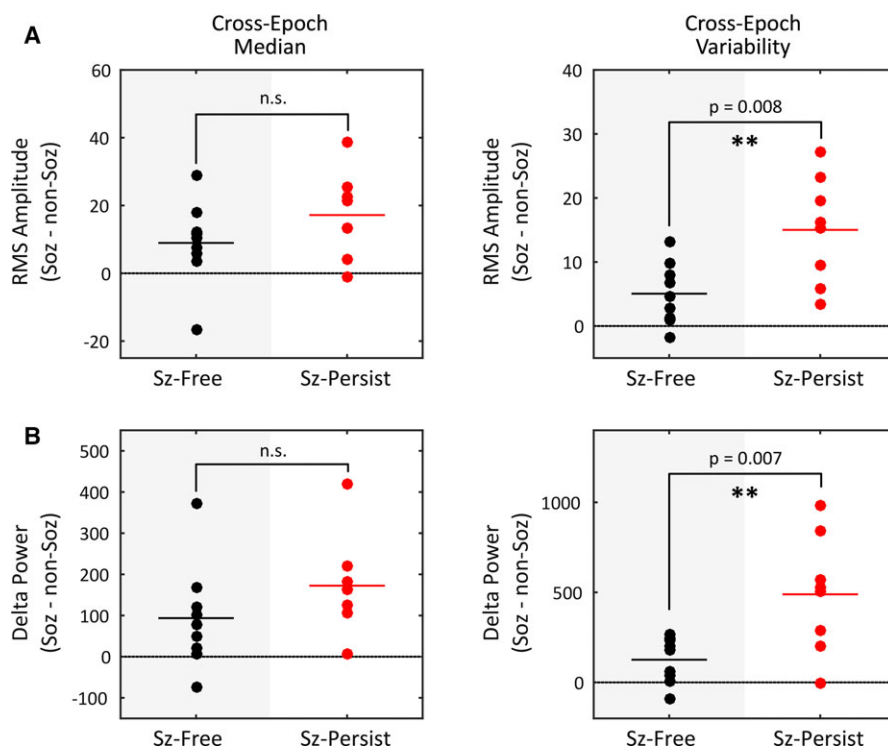
Figure 3.

Increased global synchrony characterizes patients with seizure-persistent outcomes. **(A)** Average functional connectivity matrices from eight representative patients are shown (Sz-Free: patients 01, 05, 11, and 14; Sz-Persist: patients 02, 04, 09, and 12). Warm colors (yellow) correspond to increased connection weights. Visual inspection suggests that global connectivity strength is increased among Sz-Persist patients. **(B)** *Left:* The average of the off-diagonal matrix entries (mean connectivity strength) was significantly greater in Sz-Persist patients compared to Sz-Free patients. *Middle:* Cumulative probability distributions (CPDs) encoding the distribution of off-diagonal matrix entries were averaged for Sz-Free and Sz-Persist patients (edge weight increment = 0.005). *Right:* Functional Data Analysis (FDA) was used to compare Sz-Free and Sz-Persist CPD curves. The observed curve difference exceeded 99.2% of the permutation distribution (gray), yielding a p-value of 0.008.

Epilepsia © ILAE

density was observed between Sz-Persist (2.97 ± 1.81 spikes/chan/min) and Sz-Free (2.05 ± 1.74 spikes/chan/min) groups ($p = 0.30$). Across all patients, the linear

correlation (Pearson, r^2) between interictal spike density and global connectivity strength was not significant ($r^2 = 0.38$, $p = 0.45$).

**Figure 4.**

Increased heterogeneity of RMS amplitude and absolute delta power characterize the SOZ in Sz-Persist patients only. For each patient, difference scores (SOZ – non-SOZ) were computed for the amplitude heterogeneity (left) and delta power heterogeneity (right). Sz-Persist patients exhibited increased heterogeneity difference scores of both amplitude and delta power compared to Sz-Free patients (Student's *t*-tests, $p < 0.01$).
Epilepsia © ILAE

Next, to investigate whether global connectivity differences were driven by specific regions of the recording field,²⁰ we separately examined connections between pairs of SOZ channels (SOZ–SOZ), SOZ and non-SOZ channels (SOZ–NSOZ), and non-SOZ channel pairs (NSOZ–NSOZ) (Fig. S1). No difference in mean SOZ–SOZ connectivity strength was observed between Sz-Free (0.180 ± 0.060) and Sz-Persist (0.227 ± 0.112) patients ($p = 0.33$). Similarly, no group difference was observed for mean SOZ–NSOZ connectivity (Sz-Persist: 0.082 ± 0.071 ; Sz-Free: 0.071 ± 0.083 ; $p = 0.77$). However, a significant increase in NSOZ–NSOZ connectivity strength was observed among Sz-Persist (0.167 ± 0.045) compared to Sz-Free (0.097 ± 0.032) patients ($p = 0.002$). Average CPDs of NSOZ–NSOZ edge weights were significantly different between the two outcome groups (FDA test, iterations = 10,000, $p = 0.002$) but not for the SOZ–SOZ or SOZ–NSOZ analyses (Fig. S1, lower). These findings suggest that the global connectivity differences observed between Sz-Free and Sz-Persist patients are driven primarily by connections outside of the SOZ.

Local signal heterogeneity

Local signal heterogeneity was characterized by measuring the variability of RMS amplitude and absolute delta power across epochs (Fig. 4). For both measures, difference scores (SOZ – non-SOZ) were computed for each patient by subtracting the average of SOZ channels from the average corresponding to non-SOZ channels. We observed dramatic

increases in both the amplitude heterogeneity difference score ($p = 0.008$) and the delta heterogeneity difference score ($p = 0.007$) for Sz-Persist patients compared to Sz-Free patients (Fig. 4). Thus, increased signal heterogeneity within SOZ compared to non-SOZ electrodes was a marker for seizure persistence.

Patient classification using SVM

Global synchrony and local heterogeneity measures were submitted to an SVM learning algorithm to assess whether a combination of predictors could be used to predict surgical outcome (Fig. 5). Mean connectivity strength was used as the global synchrony predictor variable. Collapsing across the two local heterogeneity difference scores using PCA yielded a first principal component (PC #1) explaining >99% of the data variance. Component scores from PC #1 were submitted as the local heterogeneity predictor. The sensitivity, specificity, and accuracy of the SVM were assessed using the LOO method and compared to permutation distributions (iterations = 10,000) to determine statistical significance.¹⁴ Based on surgical outcome, the SVM classified patients with 100% sensitivity (LOO, $p < 0.001$), 87.5% specificity (LOO, $p = 0.041$), and 94.1% accuracy (LOO, $p < 0.001$).

DISCUSSION

Epilepsy surgery has been a lynchpin in the treatment of intractable seizures for decades, but modern preoperative

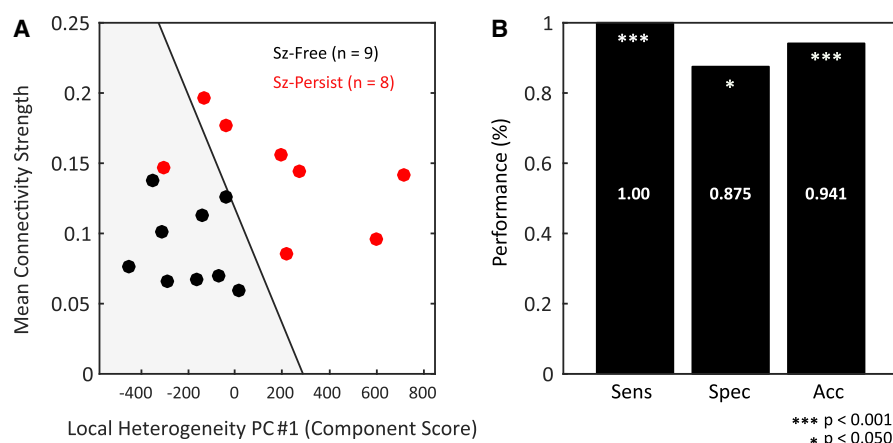


Figure 5.

SVM learning algorithm accurately assigns patients to surgical outcome groups. **(A)** Local and global synchrony measures (local: principal component #1 (PC #1) Component scores; global: Mean Connectivity Strength) were used as predictors for a linear-kernel SVM algorithm. The black line classifier is computed to optimally separate the labeled outcome groups. **(B)** The sensitivity, specificity, and accuracy of the classifier were determined using the “Leave-One-Out” (LOO) method and assessed using nonparametric permutation tests (iterations = 10,000). The sensitivity (9/9, 100%), specificity (7/8, 87.5%), and accuracy (16/17, 94.1%) of the classifier were all significantly greater than chance. One patient (Pt 03, Sz-Persist) was misclassified by the SVM as Sz-Free.

Epilepsia © ILAE

assessments are insufficient to ensure seizure-free outcomes. In this study, we investigated whether interictal IEEG activity could be used to assess risk for postsurgical seizure recurrence on an individual-patient basis. We found that measures of global network synchrony and local signal heterogeneity differed between favorable (Sz-Free) and unfavorable (Sz-Persist) outcome groups. Furthermore, a supervised learning algorithm was able to use interictal measures to predict surgical outcome with impressive accuracy (16/17, 94.1%) despite tremendous variability in patient history, implant location, and electrode configuration.

Measuring global network synchrony revealed increased mean connectivity strength in Sz-Persist patients compared to Sz-Free patients (Fig. 3). Furthermore, we found that global connectivity differences were driven primarily by increased connectivity strength outside of the SOZ (i.e., NSOZ–NSOZ) in Sz-Persist compared to Sz-Free patients (Fig. S1). Thus, diffuse synchrony across the electrode implant extending beyond the neurologist-defined SOZ was a marker for unfavorable surgical outcome. Functional connectivity within the epileptic brain has been studied extensively in recent years (see Haneef and Chiang²⁵ for review), but few studies have investigated the relationship between network connectivity and surgical outcome. One recent study by Antony et al.¹⁴ examined interictal functional EEG connectivity in 23 adult patients with TLE, finding increased global connectivity strength in seizure-persistent patients compared to seizure-free patients. This finding is consistent with the results from the present study. We note that

the congruence of the two studies is compelling given the major differences in methodology and patient population, suggesting that the relationship between connectivity strength and surgical outcome is robust to these differences. Increased global connectivity strength in Sz-Persist patients may reflect a more diffuse distribution of underlying cortical abnormalities. Indeed, the majority of Sz-Persist patients in this study exhibited nonlesional MRI presentations (7/8, 87.5%), suggesting that the epileptogenic focus is not as discrete or confined as may be observed in MRI-lesional patients. Furthermore, networks with increased global connectivity strength may be more resilient to surgical resection by offering alternate pathways for activity to spread when individual nodes are excised. Future simulation studies examining the effect of targeted node deletions on network function in seizure-free and seizure-persistent patients would provide valuable insights into this relationship between global connectivity strength and surgical outcome.

Next, local signal heterogeneity was assessed by calculating the variability of RMS amplitude and absolute delta power across epochs, and comparing heterogeneity in SOZ versus non-SOZ electrodes. We found increased signal heterogeneity in SOZ electrodes compared to non-SOZ electrodes, primarily among Sz-Persist patients (Fig. 4). Increased signal heterogeneity within the SOZ may reflect the presence of transient bursts of high amplitude, focal slow activity intermittent with periods of low amplitude fast activity. Both signal features have been linked extensively to the SOZ, whereas regional delta bursts are thought to implicate thalamocortical projection neurons.²⁶ Indeed,

considering the epileptogenic network extending into subcortical structures differentially in Sz-Persist (but not Sz-Free) patients can explain the two separate quantitative findings of this study. Although this is not directly clinically testable because patients with subcortical extension of the epileptogenic network do not undergo resection, this reasoning aligns with the increased signal heterogeneity in SOZ versus non-SOZ channels in seizure-persistent patients (Fig. 4). We propose that subcortical network nodes serve as “common source” inputs driving highly synchronous oscillations across the cortical surface,¹⁸ leading to elevated synchrony in both SOZ and non-SOZ regions (i.e., consistent with the findings among Sz-Persist patients). Although the present results support the subcortical extension model of seizure persistence, future research is needed to adequately scrutinize this hypothesis.

The global synchrony and local heterogeneity analyses yielded synergistic insights regarding the interictal organization of epileptic networks across outcome groups, with both findings pointing to more diffuse network abnormalities in Sz-Persist patients. Group differences alone, however, cannot improve presurgical management for any individual patient. Using a combination of local and global measures, we demonstrate that a linear-kernel SVM algorithm accurately classified 16 (94.1%) of 17 patients by surgical outcome (Fig. 5A). Although 100% accuracy was not observed in this study, the classifier performed exceptionally well at classifying individual patients given the variability of the dataset. In the study by Antony et al.,¹⁴ researchers trained an SVM learning algorithm that predicted surgical outcome with accuracy similar to the present method (87%). However, the patient cohort in that study was limited to adult TLE patients with consistent IIEG implants who ultimately received a standard temporal lobectomy. In this study, we observed strong predictive performance of the SVM classifier despite tremendous variability in the presentation and surgical management of the examined patients. We therefore expect the present methodology to generalize to a diverse range of epilepsy patients.

When evaluating the utility of our EEG-based methodology, it is important to note that several clinical variables in the study were strongly associated with surgical outcome (Table S1). For instance, the presence or absence of MRI-visible cortical lesions predicted surgical outcome but did not reach the performance of the EEG-based algorithm (MRI 13/17, 76.5% vs. EEG 16/17, 94.1%). This finding is consistent with previous studies demonstrating that nonlesional MRI imaging is correlated with unfavorable epilepsy surgery outcomes among pediatric patients.^{8,27} The improved accuracy of our method suggests that our novel interictal methodology is sensitive to group differences that are not captured by more traditional clinical variables. Future studies will combine both clinical variables and signal processing to develop robust, multivariate outcome prediction models.

Despite the promising results of this study, future investigation is needed to address limitations and further define the clinical utility of the method. For instance, although the classifier performed extremely well, one seizure-persistent patient (patient 03) was misclassified as seizure-free. This patient exhibited mean connectivity strength similar to other Sz-Persist patients but resembled the Sz-Free group with regard to the local heterogeneity measures. Because difference scores between SOZ and non-SOZ electrodes were used in calculating the local heterogeneity predictor, it is possible that the epileptogenic focus was undersampled during the implant, leading to erroneous SOZ – non-SOZ difference scores. Incorporating additional predictor variables that do not require SOZ – non-SOZ comparisons may allow for accurate classification of this patient. Alternatively, increased sampling of the brain may improve the performance of the classifier.

Other limitations include the lack of consideration for several temporal variables (e.g., time of day, sleep and wake state, proximity to seizures) in our analysis. The use of a random and large number of epochs per patient ($n = 1,200$) presumes that the epochs were distributed evenly between the two outcome groups and any temporal contribution would be averaged across the data. Future analysis could better assess if these temporal features would improve the accuracy of our measure. Finally, for this initial investigation, an amplitude-based correlation technique was used to characterize functional connectivity because the simplicity and efficiency of these methods are well-suited for the clinical setting. Considering that many techniques can be used to characterize EEG connectivity, replicating our global connectivity findings using a phase-based connectivity approach (e.g., spectral coherence) may bolster the generalizability of the study. Based on previous research finding similar performance between amplitude-based and phase-based connectivity methods,^{28–30} we predict that the results would not noticeably change using a different measure of functional connectivity.

In the present study, we examined interictal network synchrony in pediatric IIEG patients with drug-resistant epilepsies. We identified robust differences in global synchrony and local heterogeneity measures that were sufficient to predict surgical outcome with impressive accuracy. These findings suggest that the organization of the epileptogenic zone and the distribution of the underlying cortical abnormalities can be reliably assayed from presurgical recordings, thereby contributing useful information to neurologists assessing surgical candidacy.

ACKNOWLEDGMENTS

The first author was supported by funding from the American Association of Neurological Surgeons (AANS) and the Neurosurgery Research and Education Foundation (NREF). Additional funding for this project was provided by the Children's Hospital Women's Committee. The authors thank Drs. Gregory Heuer and Jay Storm (CHOP) for their collaboration in this

study, Thuy-My Le (CHOP) for her review of the manuscript, and Dr. Christopher Vecsey (Swarthmore College) for his thoughtful conversations. Finally, the authors are indebted to the patients and families who participated in this study.

DISCLOSURE

We confirm that we have read the Journal's position on issues involved in ethical publication and affirm that this report is consistent with those guidelines. None of the authors has any conflict of interest to disclose.

REFERENCES

- Lemieux L, Daunizeau J, Walker MC. Concepts of connectivity and human epileptic activity. *Front Syst Neurosci* 2011;5:12.
- Kramer MA, Cash SS. Epilepsy as a disorder of cortical network organization. *Neuroscientist* 2012;18:360–372.
- Palva S, Palva JM. Discovering oscillatory interaction networks with M/EEG: challenges and breakthroughs. *Trends Cogn Sci* 2012;16:219–230.
- Spencer SS. Neural networks in human epilepsy: evidence of and implications for treatment. *Epilepsia* 2002;43:219–227.
- Lüders HO, Najm I, Nair D, et al. The epileptogenic zone: general principles. *Epileptic Disord* 2006;8(Suppl. 2):S1–S9.
- Ryvlin P, Cross JH, Rheims S. Epilepsy surgery in children and adults. *Lancet Neurol* 2014;13:1114–1126.
- Moshe SL, Perucca E, Ryvlin P, et al. Epilepsy: new advances. *Lancet* 2015;385:884–898.
- Spencer S, Huh L. Outcomes of epilepsy surgery in adults and children. *Lancet Neurol* 2008;7:525–537.
- Cossu M, Lo Russo G, Francione S, et al. Epilepsy surgery in children: results and predictors of outcome on seizures. *Epilepsia* 2008;49:65–72.
- Bingaman WE, Bulacio J. Placement of subdural grids in pediatric patients: technique and results. *Childs Nerv Syst* 2014;30:1897–1904.
- Yaffe RB, Borger P, Megevand P, et al. Physiology of functional and effective networks in epilepsy. *Clin Neurophysiol* 2015;126:227–236.
- Schevon CA, Cappell J, Emerson R, et al. Cortical abnormalities in epilepsy revealed by local EEG synchrony. *NeuroImage* 2007;35:140–148.
- Ortega GJ, Menendez de la Prida L, Sola RG, et al. Synchronization clusters of interictal activity in the lateral temporal cortex of epileptic patients: intraoperative electrocorticographic analysis. *Epilepsia* 2008;49:269–280.
- Antony AR, Alexopoulos AV, Gonzalez-Martinez JA, et al. Functional connectivity estimated from intracranial EEG predicts surgical outcome in intractable temporal lobe epilepsy. *PLoS ONE* 2013;8:e77916.
- Wieser HG, Blume WT, Fish D, et al. ILAE Commission Report. Proposal for a new classification of outcome with respect to epileptic seizures following epilepsy surgery. *Epilepsia* 2001;42:282–286.
- Kramer MA, Kolaczyk ED, Kirsch HE. Emergent network topology at seizure onset in humans. *Epilepsy Res* 2008;79:173–186.
- Delorme A, Makeig S. EEGLAB: an open source toolbox for analysis of single-trial EEG dynamics including independent component analysis. *J Neurosci Methods* 2004;134:9–21.
- Cohen MX. *Analyzing neural time series data: theory and practice*. Cambridge, MA: MIT Press; 2014.
- Bassett DS, Nelson BG, Mueller BA, et al. Altered resting state complexity in schizophrenia. *NeuroImage* 2012;59:2196–2207.
- Warren CP, Hu S, Stead M, et al. Synchrony in normal and focal epileptic brain: the seizure onset zone is functionally disconnected. *J Neurophysiol* 2010;104:3530–3539.
- Bartolomei F, Bettus G, Stam CJ, et al. Interictal network properties in mesial temporal lobe epilepsy: a graph theoretical study from intracerebral recordings. *Clin Neurophysiol* 2013;124:2345–2353.
- Brown MW III, Porter BE, Dlugos DJ, et al. Comparison of novel computer detectors and human performance for spike detection in intracranial EEG. *Clin Neurophysiol* 2007;118:1744–1752.
- Tao JX, Chen XJ, Baldwin M, et al. Interictal regional delta slowing is an EEG marker of epileptic network in temporal lobe epilepsy. *Epilepsia* 2011;52:467–476.
- Palmini A, Najm I, Avanzini G, et al. Terminology and classification of the cortical dysplasias. *Neurology* 2004;62:S2–S8.
- Haneef Z, Chiang S. Clinical correlates of graph theory findings in temporal lobe epilepsy. *Seizure* 2014;23:809–818.
- Staba RJ, Worrell GA. What is the importance of abnormal “background” activity in seizure generation? *Adv Exp Med Biol* 2014;813:43–54.
- Tellez-Zenteno JF, Hernandez Ronquillo L, Moien-Afshari F, et al. Surgical outcomes in lesional and non-lesional epilepsy: a systematic review and meta-analysis. *Epilepsy Res* 2010;89:310–318.
- Ansari-Asl K, Senhadji L, Bellanger JJ, et al. Quantitative evaluation of linear and nonlinear methods characterizing interdependencies between brain signals. *Phys Rev E Stat Nonlin Soft Matter Phys* 2006;74:e031916.
- Osterhage H, Mormann F, Staniek M, et al. Measuring synchronization in the epileptic brain: a comparison of different approaches. *Int J Bifurcat Chaos* 2007;17:3539–3544.
- Andrzejak RG, David O, Gnatkovsky V, et al. Localization of epileptogenic zone on pre-surgical intracranial EEG recordings: toward a validation of quantitative signal analysis approaches. *Brain Topogr* 2015;28:832–837.

APPENDIX

Eq. A1.1: Spearman zero-lag rank correlation coefficient. For two ranked time-series x and y with n data points each, the Spearman correlation coefficient (r) is computed as:

$$r = \frac{\sum_{t=1}^n (x_t - \mu_x)(y_t - \mu_y)}{\sqrt{\sum_{t=1}^n (x_t - \mu_x)^2 \sum_{t=1}^n (y_t - \mu_y)^2}} \quad (\text{A1.1})$$

Eq. A1.2: Root mean square (RMS) amplitude. Given a time-series x with n data points, the root mean square (RMS) of x is defined as:

$$\text{rms} = \sqrt{\frac{1}{n} (x_1^2 + x_2^2 + x_3^2 + \dots + x_n^2)} \quad (\text{A1.2})$$

SUPPORTING INFORMATION

Additional Supporting Information may be found in the online version of this article:

Figure S1. Connectivity strength between pairs of SOZ channels (SOZ–SOZ), SOZ and non-SOZ channels (SOZ–NSOZ), and non-SOZ channel pairs (NSOZ–NSOZ) was examined.²⁰

Table S1. Relationship between clinical variables and surgical outcome.